AAS 21-286

SECULAR DYNAMICS BASED FEATURES FOR THE CHARACTERIZATION OF SMALL DEBRIS CLOUDS AFTER FRAGMENTATION

Di Wu[*], Aaron J. Rosengren[†]

Characterizing space debris fragmentation event, the most frequently happening debris generating event, is vital for a better understanding over the past, current, and future space environment. Limited space surveillance resources inevitably results in a lagged coverage of such event, thus requiring further detailed analysis over individual case. In addition, the chaotic feature of fragmentation would render a complex dynamics condition for the generated space debris cloud. In this research, we proposed a method to specify a reduced number of space debris from the whole space debris cloud generated by chaotic fragmenting; selected space debris are used to trace back breakup event. This method could avoid the chaotic performance induced by fragmenting while dramatically reduce calculations in backward propagation.

INTRODUCTION

Multiple fragment generation events have been documented. The most famous one is between Cosmos 2251 and Iridis 33 in 2009 as it is the first collision between two space objects. There are multiple collisions between object and debris, i.e. COSMOS 1934 spacecraft and cataloged debris 13475 (1991), CERISE spacecraft and cataloged debris 18208 (1996), THOR BURNER 2A rocket body and cataloged debris 26207 (2005), COSMOS 2251 and IRIDIUM 33 spacecraft.[1] Moreover, it has been pointed out that fragment generation event will be the major contributor of space debris in the future.[2] Space debris clouds are the result of those fragment generation events. Therefore, it is important to illustrate and characterize those space debris clouds in order to predict their evolution and possible collision scenarios.

Fragmentation event shares common problems with other topics in SSA (space situation awareness). One of them is the scarcity of data. This is both due to the huge numbers of objects needed to be tracked and the limited resources around the world that could be used. A typical data update rate is 1-2 days per update. Comparing to LEO objects' around 100-minute orbital period, this update rate is not fast enough. Another problem is the superfluity of data. While for single object we are having the problem of not enough data, we need to notice that there are huge amounts of data and information but that, in SSA, there is still a lot of dynamic ambiguity. Figuring out how to correctly extract, select, and process useful information could be valuable for some SSA problems.

Breakup event detection is an important research aspect of SSA. Researchers are inspired by seminal work from comets, asteroids, and meteors research. Dimare, etc..[3] compared several or-

[*]Graduate Student, Mechanical and Aerospace Engineerg, University of California San Diego, La Jolla, 92093.
[†]Assistant Professor, Mechanical and Aerospace Engineerg, University of California San Diego, La Jolla, 92093.

bit distance criteria and showed promising results. Tetreault, etc..[4] studied the effect of variable ballistic coefficients in the back propagating which is a key aspect of breakup event estimation.

Breakup event is highly chaotic. Space debris from a breakup event could vary dramatically in terms of their orbital elements both with respect to the original parent object right before the fragmentation and to each other in the space debris cloud. Most breakup detection algorithm would take as many debris information as possible either in simulation or in practice, and it is expected that as long as the majority would have similar orbits comparing to the parent object, the influence of minor objects could be neglected. This has been proven practical but the computational cost grows exponentially as, in the orbital distance calculation step at each time instance in the process of backwards propagation, there is a calculation of the number of combinations of n items taken 2 at a time. This number n is normally in the scale of hundreds in a normal breakup event. What's more, this computation needs to be repeated thousands of time, if not more, depends on the time step used in examining the breakup event in the back-propagation stage.

This paper presents a way to reduce the number of space debris for fast and accurate breakup event estimation. This method, inspired by asteroids and meteor breakup event estimation, applied proper elements and its related distance criteria as a pre-processing criteria to select debris objects from a huge space debris cloud. In the following paper, we first introduce the concept of proper elements and distance in proper elements space; then, we show three common orbital distance criteria frequently used in breakup event estimation; next, we introduce our pre-processing criteria, multiple numerical cases are shown with analysis afterwards; last but not least, we conclude our paper.

PROPER ELEMENTS AND PROPER ELEMENTS DISTANCE

Proper elements are first introduced in asteroids dynamics by Hirayama following his seminal study of asteroid families.[5] For the same purpose, both proper elements distance and clustering methods are further developed.

Proper Elements

Proper elements are quasi-integrals of motion, representing the covered "signature" of a space object. In our current definition, there are three elements in proper elements, respectively proper semi-major axis, proper eccentricity, and sine of proper inclination. While the physical meaning of proper semi-major axis is similar to semi-major axis in the context of both osculating (orbital) elements and mean (orbital) elements, the physical meaning of either proper eccentricity or sine of proper inclination is distinct from its counterparts in mean elements, let along osculating elements.

We define proper semi-major axis to be the averaged semi-major axis during the whole time span that we are considering for proper elements; this time span is normally several thousand orbit revolutions as it is related to the definition of proper eccentricity and sine of proper inclination. For proper eccentricity and sine of proper inclination explanation, we start by taking a modified equinoctial elements conversion from classical orbit elements $(a, e, i, \Omega, \omega, M)$ as Eq. (1). In their separate spaces, either (k, h) or (p, q), with a specified perturbation model, the solution trajectories, as shown in Fig. 1, are composed of a frozen component subscribed by f and a proper component subscribed by p. While the frozen component is fixed in specified space (either (k, h) or (p, q)) and related to only the semi-major axis of a space object, the proper component would rotate along the way that solution trajectory follows, but with a constant magnitude which is decided by the initial

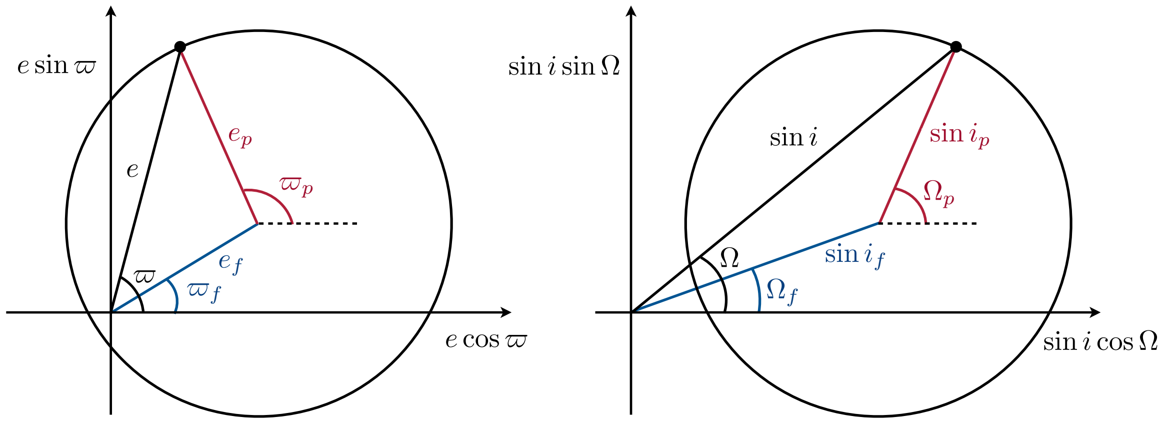

Figure 1: Orbit evolution is expressed as two solution trajectories in (k, h) and (p, q) space separately with proper component subscribed by p, i.e. $e_p,\ \varpi_p,\ \sin i_p,\ \Omega_p$ and frozen component subscribed by f, i.e. $e_f,\ \varpi_f,\ \sin i_f,\ \Omega_f$.

condition of the corresponding space object's orbit.

$$\begin{aligned} &k = e \cos \varpi,\ h = e \sin \varpi \\ &p = \sin i \cos \Omega,\ q = \sin i \sin \Omega \\ &\text{where } \varpi = \Omega + \omega \end{aligned} \tag{1}$$

The way of uncovering proper elements from modeling space object's orbital evolution, either numerically or analytically, would introduce some kind of model simplification into the process,[6] but the important feature would persist: proper elements are quasi-constant representations of orbit. This means: proper elements experiences negligible change comparing to mean elements or osculating elements in terms of both value and time.

A 100-day orbit evolution under high order Earth harmonic perturbation is shown in Fig. 2. Its osculating elements and mean elements in terms of the corresponding $(e, \sin i)$ parts are sampled. We calculate its proper elements counterparts under a zonal-only harmonic perturbation model, following Walter's book.[7] Proper elements almost crumbled together while its mean and osculating counterparts scattered around the $(e, \sin i)$ space, covering a much larger area.

We refer to Wu and Rosengren's work[8] for the detailed procedure of calculating proper elements from osculating elements at each time instance.

Proper Elements Distance

Proper elements distance is essential to study the connections among a group of space objects. It arises from the necessity of defining similarity between objects in proper elements space. Astronomers have used such criteria to define asteroids families.

One way of defining proper elements distance is through a function, denoted by $d_{Cellino}$, in the proper elements space, as shown in Eq. (2), where $k_1 = 5/4,\ k_2 = 2,\ k_3 = 2$.

$$d_{Cellino} = n_{ave} a_{ave} \sqrt{k_1(\delta a / a_{ave})^2 + k_2(\delta e)^2 + k_3(\delta i)^2} \tag{2}$$

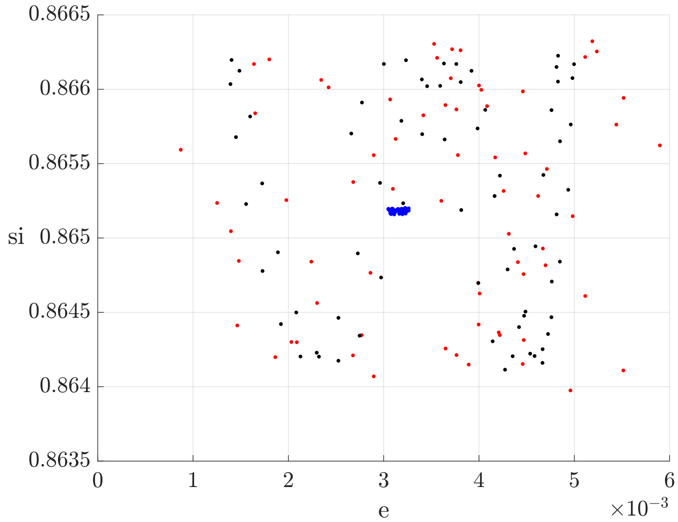

Figure 2: Space differences for osculating elements (red), mean elements (black), and proper elements (blue) in $(e, \sin i)$ space are shown for a 100-day test scenario.

For a pair of proper elements $\boldsymbol{p}œ_A$, $\boldsymbol{p}œ_B$, where $\boldsymbol{p}œ = (a_p, e_p, \sin i_p)$. a_{ave} is the average between them $a_{ave} = (a_{p,A} + a_{p,B})/2$; n_{ave} is the corresponding angular velocity $n_{ave} = \sqrt{\mu/a_{ave}^3}$ for Earth's gravitational parameter μ; δa is the difference in proper semi-major axis $\delta a = a_{p,A} - a_{p,B}$; similarly $\delta e = e_{p,A} - e_{p,B}$ and $\delta i = i_{p,A} - i_{p,B}$ with transformation $i_p = \sin^{-1}(\sin i_p)$.

We refer the work from Zappala and Cellino, etc..[9] for detailed derivation and explanation of the proper elements distance criteria $d_{Cellino}$.

ORBITAL DISTANCES

Orbital distance is the characterization of similarity between two orbits. Two highly similar orbits, at a given time instance, are also highly likely to belong to the same object. For more orbits, the averaged value among all possible pairs of orbits is used to characterize orbital distance for the whole group. In the context of debris breakup event, at the breakup time, the similarity for a group of space debris from this event should be the highest, i.e. a global extremum, in the orbital distance evolution.

In this work, we use the classical keplerian orbital elements to define orbit $œ_A$ and orbit $œ_B$ in Eq. (3) with semimajor axis a, eccentricity a, inclination i, ascending node Ω, argument of perigee ω, and mean anomaly M.

$$
\begin{aligned}
œ_A &= (a_A, e_A, i_A, \Omega_A, \omega_A, M_A) \\
œ_B &= (a_B, e_B, i_B, \Omega_B, \omega_B, M_B)
\end{aligned}
\tag{3}
$$

The selection of orbital distance is critical to correctly estimate when breakup event happens. The work from Dimare, etc..[3]shows that orbital distance proposed by Southworth and Hawkins[10] and orbital distance proposed by Jopek[11] could effectively detect breakup event. We notify that MOID (minimal orbit intersection distance) and nodal distance could detect the breakup event as well, but at a much larger computational cost.[3] In addition, their results indicate that if a breakup event could be detected by MOID or nodal distance, orbital distance by Southworth and Hawkins and by Jopek could also detect it with a reasonable accuracy. So, we choose the orbital distance proposed by Southworth and Hawkins and orbital distance proposed by Jopek as the criteria to estimate orbital distance in our work.

The orbital distance by Southworth and Hawkins, denoted by d_{SH}, is defined by Eq. (4).

$$d_{SH}^2 = (e_B - e_A)^2 + \frac{(q_B - q_A)^2}{R_{\text{Earth}}^2} + \left(2\sin\left(\frac{I_{BA}}{2}\right)\right)^2 + \left(\frac{e_B + e_A}{2}\right)^2 \left(2\sin\left(\frac{\pi_{BA}}{2}\right)\right)^2 \quad (4)$$

q is the semi-latus rectum $q = a(1-e^2)$; R_{Earth} takes the equatorial radius of Earth; I_{BA} is the orbital inclination difference, calculated by finding the angle difference between two orbits' unit angular momentum vectors $\hat{h}_A, \hat{h}_B$ as shown in Eq. (5), where $\hat{h} = \sin i \ sin\Omega \, \hat{x} - \sin i \cos\Omega \, \hat{y} + \cos i \, \hat{z}$ in the ECI frame denoted by $(\hat{x}, \hat{y}, \hat{z})$;

$$I_{BA} = \cos^{-1}(\hat{h}_A \cdot \hat{h}_B) \quad (5)$$

π_{BA} is the difference between two longitudes of perigees measured from the intersection of the orbits; its equation is shown in Eq. (6).

$$\begin{aligned} \pi_{BA} &= \omega_B - \omega_A + 2\sin^{-1}(S_{BA}) \\ S_{BA} &= \cos\left(\frac{i_B + i_A}{2}\right) \sin\left(\frac{\Omega_B - \Omega_A}{2}\right) \sec\frac{I_{BA}}{2} \end{aligned} \quad (6)$$

The orbital distance by Jopek, denoted by d_J, is defined by Eq. (7).

$$d_J^2 = (e_B - e_A)^2 + \left(\frac{q_B - q_A}{q_B + q_A}\right)^2 + \left(2\sin\left(\frac{I_{BA}}{2}\right)\right)^2 + \left(\frac{e_B + e_A}{2}\right)^2 \left(2\sin\left(\frac{\pi_{BA}}{2}\right)\right)^2 \quad (7)$$

Orbital distance by Jopek d_J shares the parameters definition of semi-latus rectum q, inclination difference I_{BA}, and difference between two longitudes of perigees measured from the intersection of the orbits π_{BA} with orbital distance by Southworth and Hawkins d_{SH}.

Last but not least, the orbital distance criteria by Zappala and Cellino $d_{Cellino}$ as defined before is also used as an orbital distance in osculating space.

PRE-PROCESSING METHOD AND NUMERICAL TEST

Suppose we have a cloud of fragments with known properties and orbits for a limited time instances t_k, t_{k+1}, t_{k+2}, t_{k+3}, for debirs objects at each time instance, for example at t_k, we would calculate their corresponding proper elements and choose a limited number N_p of pairs of closest objects in terms of proper elements distance. A list of chosen objects l_k for this time instance is recorded. Then, this process is repeated for all time instances. At the end, out of all chosen objects in lists l_k, l_{k+1}, l_{k+2}, l_{k+3}, we would select those objects that appear on all those lists and create a new list l_s. Only those space objects on the l_s list are back-propagated for the breakup event estimation.

In the numerical test, we used NASA's Standard Breakup Model[12] to generate a reasonable space debris cloud in LEO region. High fidelity propagator `THALASSA`[13] was employed to have initial condition propagated forward for 10 days. We assumed a full data covering every space debris could

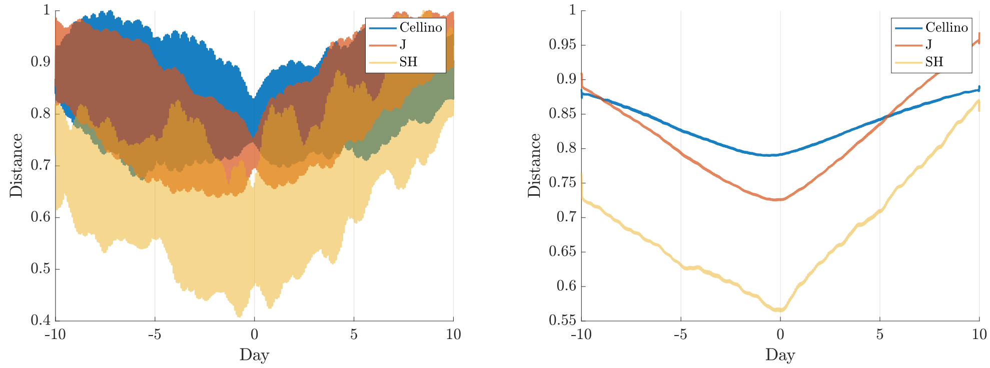

Figure 3: Orbital distances results following criteria $d_{Cellino}$, d_J, d_{SH} for objects in l_s list. Both plots show a successful detection of breakup event at Day 0. **left**: selected objects' scaled orbital distances results. **right**: smoothed, by a 20 data moving average filter, orbital distances results.

be acquired every 2.5 days. The parameters for initial conditions creation is shown in Table 1 where drag coefficient is set to be 2.1 and SRP (solar radian pressure) coefficient 1.2.

Following the pre-processing described before, we find the l_s list of space objects. There are 119 objects selected from 1180 original objects. If all 1180 objects are used in back-propagation, there are $C_{1180}^2 = 695610$ operations simply in the comparison stage for each instance; now for 119 objects, there are only $C_{119}^2 = 7021$ operations, about 1% of all objects case. The operations are also saved in the back-propagation as there are less objects to propagate.

We use the final states from our modeled pseudo-observation and set the back-propagation to be 20 days at a time interval of around 5 minutes. The breakup event detection result from l_s is shown in Fig. 3. We could successfully estimate the breakup event accurately either from the non-smoothed **left** figure or from the smoothed **right** figure, as the minimum parts of both plots are around the correct Day 0 breakup time.

For comparison, we conducted a random selection of 120 objects, a similar number to objects in l_s list, from the original data. The result is shown in Fig. 4. While the non-smoothed **left** figure could give a good estimation, the smoothed **right** figure, which should give a confirmation result, would give a wrong estimation.

We also examined our method under various independent white noise in $\boldsymbol{RSW}$ frame as listed in Table 2. The result of case i is shown in Fig. 5, and the result of case e is shown in Fig. 6. Under case i white noise, while all three curves for different criteria changed in the process, comparing to original case in 3, due to the white noise, we could still have a good estimation of the breakup event. However, under case e, we could start to see the influence of white noise over the estimation of breakup event.

Table 1: Initial conditions for debris cloud generation. L_c is the characteristic length parameter and N the number parameter in NASA Standard Breakup Model.

MJD	$a(km)$	e	$i(°)$	$\Omega(°)$	$\omega(°)$	$M(°)$	N	$L_c(m)$
58675	7800	0.0015	80.3	24.0	345.0	32.0	1180	0.1

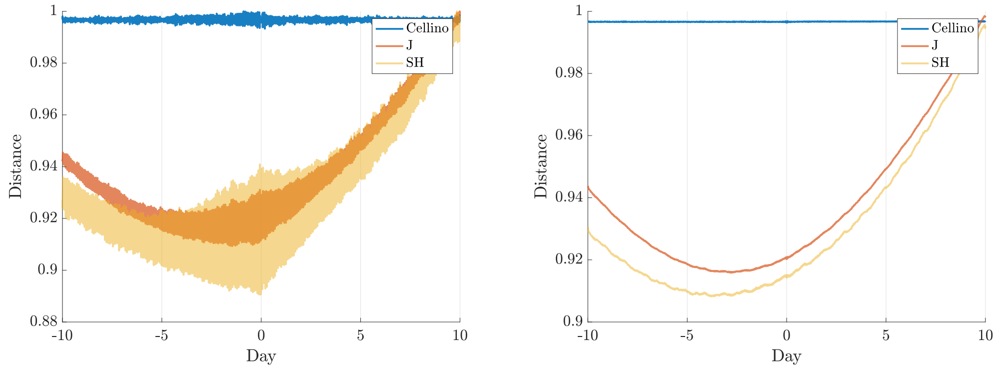

Figure 4: Orbital distances results following criteria $d_{Cellino}$, d_J, d_{SH} for randomly selected 120 objects. While **left** figure could argue about the correct breakup event estimation, **right** figure, which should give a confirmation result, would give a missed estimation. **left**: selected objects' scaled orbital distances results. **right**: smoothed, by a 20 data moving average filter, orbital distances results.

Table 2: Case i and case e of white noise in $\boldsymbol{RSW}$ frame.

label	$\sigma_x(m)$	$\sigma_y(m)$	$\sigma_z(m)$	$\sigma_{vx}(m/s)$	$\sigma_{vy}(m/s)$	$\sigma_{vz}(m/s)$
case i	0.01	0.03	0.02	0.0001	0.0001	0.0001
case e	0.1	0.3	0.2	0.001	0.001	0.001

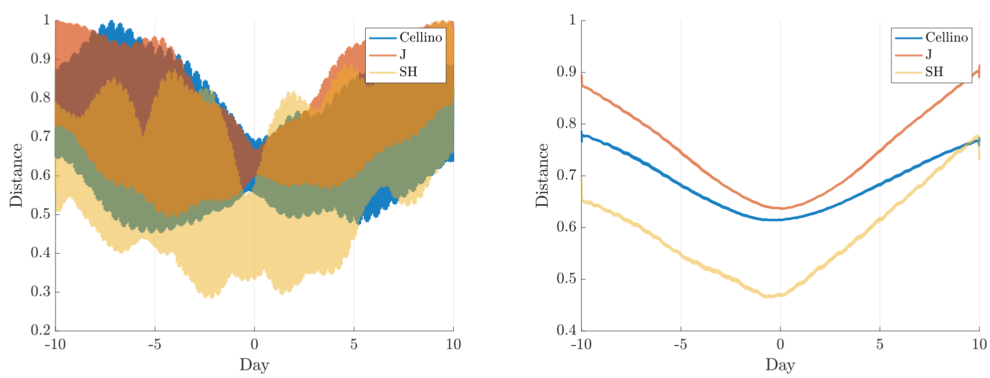

Figure 5: Orbital distances results following criteria $d_{Cellino}$, d_J, d_{SH} for objects in l_s list under white noise condition case i in Table 2. The correct breakup estimation is influenced in this case. **left**: selected objects' scaled orbital distances results. **right**: smoothed, by a 20 data moving average filter, orbital distances results.

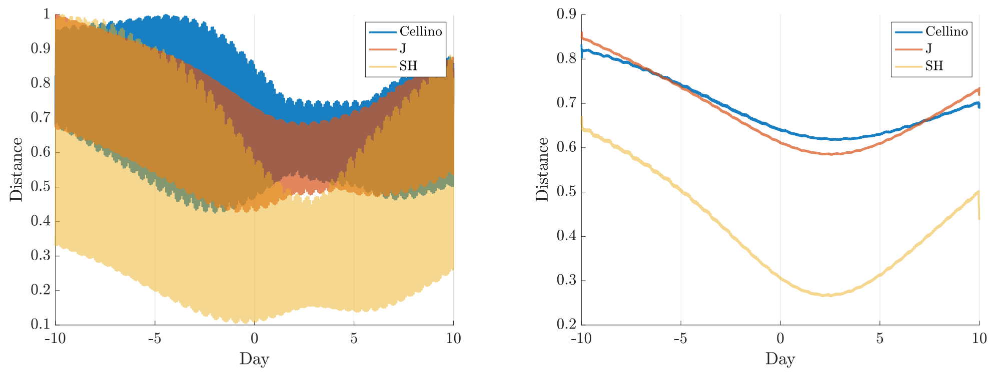

Figure 6: Orbital distances results following criteria $d_{Cellino}$, d_J, d_{SH} for objects in l_s list under white noise condition case e in Table 2. The correct breakup estimation is influenced in this case. **left**: selected objects' scaled orbital distances results. **right**: smoothed, by a 20 data moving average filter, orbital distances results.

CONCLUSION

This study develops a pre-processing method based on proper elements to trace back breakup event. The proposed method greatly reduces the computational requirement while providing effective estimation ability. Out of the chaotic debris cloud generated by a breakup event, our proposed method tracks down the objects that could provide less confusing and more valuable information about the breakup event from an astrodynamics point of view. Lastly, We investigate the influence from orbit uncertainty. Although orbit uncertainty would change the detailed performance of our method, to some extent, we could still apply the same method. Future study would needs to evaluate orbit uncertainty's influence for both pre-processing stage and back-propagation stage.

REFERENCES

[1] B. Zhang, Z. Wang, and Y. Zhang, "An analytic method of space debris cloud evolution and its collision evaluation for constellation satellites," *Advances in Space Research*, Vol. 58, Sept. 2016, pp. 903–913, 10.1016/j.asr.2016.03.016.

[2] J.-C. Liou and N. L. Johnson, "Risks in Space from Orbiting Debris," *Science*, Vol. 311, Jan. 2006, pp. 340–341, 10.1126/science.1121337.

[3] L. Dimare, S. Cicalò, A. Rossi, E. M. Alessi, and G. Valsecchi, "In-Orbit Fragmentation Characterization and Parent Bodies Identification by Means of Orbital Distances," 12 2019.

[4] K. Tetreault, S. Ross, K. Schroeder, and J. Black, "Fragmentation Event Identification Using Back Propagation with Variable Ballistic Coefficient Calculation," 2018.

[5] K. Hirayama, "Groups of asteroids probably of common origin," *The Astronomical Journal*, Vol. 31, Oct. 1918, p. 185, 10.1086/104299.

[6] Z. Knezevic, A. Lemaître, and A. Milani, "The Determination of Asteroid Proper Elements," *Asteroids III*, 01 2002.

[7] U. Walter, *Astronautics*. Springer International Publishing, 2018, 10.1007/978-3-319-74373-8.

[8] D. Wu and A. J. Rosengren, "analysis of proper orbital element for resident space objects," IAC-19, 2019.

[9] V. Zappala, A. Cellino, P. Farinella, and Z. Knezevic, "Asteroid families. I - Identification by hierarchical clustering and reliability assessment," *The Astronomical Journal*, Vol. 100, Dec. 1990, p. 2030, 10.1086/115658.

[10] R. B. Southworth and G. S. Hawkins, "Statistics of meteor streams," *Smithsonian Contributions to Astrophysics*, Vol. 7, Jan. 1963, pp. 261–285.

[11] T. J. Jopek, “Remarks on the Meteor Orbital Similarity D-Criterion,” *Icarus*, Vol. 106, Dec. 1993, pp. 603–607, 10.1006/icar.1993.1195.

[12] N. Johnson, P. Krisko, J.-C. Liou, and P. Anz-Meador, “NASA's new breakup model of evolve 4.0,” *Advances in Space Research*, Vol. 28, Jan. 2001, pp. 1377–1384, 10.1016/s0273-1177(01)00423-9.

[13] D. Amato, C. Bombardelli, G. Baù, V. Morand, and A. J. Rosengren, “Non-averaged regularized formulations as an alternative to semi-analytical orbit propagation methods,” *Celestial Mechanics and Dynamical Astronomy*, Vol. 131, May 2019, 10.1007/s10569-019-9897-1.